Atmospheric Environment 43 (2009) 4603–4611

Contents lists available at ScienceDirect

Atmospheric Environment

journal homepage: www.elsevier.com/locate/atmosenv

The sensitivity of modeled ozone to the temporal distribution of point, area, and mobile source emissions in the eastern United States

Patricia Castellanos [a], Jeffrey W. Stehr [b], Russell R. Dickerson [b], Sheryl H. Ehrman [a,*]

[a] Department of Chemical and Biomolecular Engineering, 2113 Bldg 90, University of Maryland, College Park, MD 20742, USA
[b] Department of Atmospheric and Oceanic Science, University of Maryland, 2113 Bldg 90, College Park, MD 20742, USA

ARTICLE INFO

Article history:
Received 20 February 2009
Received in revised form
12 May 2009
Accepted 22 May 2009

Keywords:
Modeling
Air pollution
Emissions
Ozone

ABSTRACT

Ozone remains one of the most recalcitrant air pollution problems in the US. Hourly emissions fields used in air quality models (AQMs) generally show less temporal variability than corresponding measurements from continuous emissions monitors (CEM) and field campaigns would imply. If emissions control scenarios to reduce emissions at peak ozone forming hours are to be assessed with AQMs, the effect of emissions' daily variability on modeled ozone must be understood. We analyzed the effects of altering all anthropogenic emissions' temporal distributions by source group on 2002 summer-long simulations of ozone using the Community Multiscale Air Quality Model (CMAQ) v4.5 and the Carbon Bond IV (CBIV) chemical mechanism with 12 km resolution. We find that when mobile source emissions were made constant over the course of a day, 8-h maximum ozone predictions changed by ±7 parts per billion by volume (ppbv) in many urban areas on days when ozone concentrations greater than 80 ppbv were simulated in the base case. Increasing the temporal variation of point sources resulted in ozone changes of +6 and −6 ppbv, but only for small areas near sources. Changing the daily cycle of mobile source emissions produces substantial changes in simulated ozone, especially in urban areas at night; results suggest that shifting the emissions of NO_x from day to night, for example in electric powered vehicles recharged at night, could have beneficial impacts on air quality.

1. Introduction

Ozone concentrations exceeding the 0.08 parts per million by volume (ppmv) 8-h average National Ambient Air Quality Standard (NAAQS) are a longstanding problem in many Northeast urban/suburban areas (USEPA, 2004). Ozone is formed from a complex set of photochemical reactions involving nitrogen oxides (NO_x) and volatile organic compounds (VOCs) that is driven by high temperatures and sunlight (Seinfeld and Pandis, 2006). Now that the 75 parts per billion by volume (ppbv) 8-h average standard has been put forth, there is additional pressure on policy makers to create effective emissions control strategies for these precursors on a local and regional level. Because NO_x emissions have decreased significantly following the U.S. Environmental Protection Agency's (EPA) NO_x State Implementation Plan (SIP) call and the introduction of lower emitting vehicles to the fleet (Bloomer et al., 2009) many regulators are focusing on reducing emissions at peak ozone forming hours. For example, in 2007 the states of the Ozone Transport Commission (OTC) signed a memorandum of understanding to reduce NO_x emissions from peaking units on high electrical demand days (HEDD). These units are otherwise largely unregulated, often the dirtiest units in the region, and operate on the hottest days of the year.

Air quality models (AQMs) that simulate chemistry, transport and diffusion, and atmospheric removal processes of multiple pollutants including trace gases and aerosols, are an important tool for studying ozone. They have been used for decision support, regulatory attainment analysis, creation of emissions control strategies and experiments in atmospheric chemistry and transport. Although in many instances AQMs satisfactorily replicate ozone when compared to surface observations the simulations are subject to uncertainty resulting from parameterizations and approximations embedded in the model algorithms and chemical mechanisms, as well as inaccuracies in the meteorological and emissions inputs (Hanna et al., 1998; Placet et al., 2000; Bey et al., 2001; Fine et al., 2003; Brunner et al., 2005; Arnold and Dennis, 2006; Eder and Yu, 2006; Mallet and Sportisse, 2006; Appel et al., 2007; Gego et al., 2008; Godowitch et al., 2008).

Emissions inventories, reported as annual or daily average values, must be broken up into the hourly fluxes required by AQMs using generalized temporal distributions. The resulting estimate of

* Corresponding author. Tel.: +1 301 405 1917.
E-mail addresses: patti@umd.edu (P. Castellanos), stehr@atmos.umd.edu (J.W. Stehr), russ@atmos.umd.edu (R.R. Dickerson), sehrman@umd.edu (S.H. Ehrman).

1352-2310/$ – see front matter © 2009 Elsevier Ltd. All rights reserved.
doi:10.1016/j.atmosenv.2009.05.045

hourly emissions that are AQM inputs are less variable than corresponding measurements from continuous emissions monitors (CEM) and field campaigns would imply (Placet et al., 2000; Hanna et al., 1998; Marr et al., 2002; Murphy and Allen, 2005). Emission rates from peaking units, for instance, are currently not well represented in the model. Before going to the expense of creating inventories that represent real world variability, we would like to know how sensitive the model is to the temporal variability of emissions. This will give us an idea of the magnitude of results to expect from implementing detailed emissions control strategies that target time of day.

Webster et al. (2007) created a stochastic emissions inventory of industrial VOC emissions to better represent large magnitude emissions events in the Houston–Galveston area. Using a fine grid (1 km) over the Houston–Galveston area, they compared the stochastic inventory to an inventory with constant industrial emissions and found that increased variability created changes in hourly ozone concentration in the range of 10–52 ppb. Nam et al. (2008) demonstrated that applying controls to the stochastic emissions is more effective at reducing the highest ozone concentrations than controlling constant emissions.

Tao et al. (2004) compared a simulation with constant anthropogenic emissions (uniform temporal profiles) to a simulation where anthropogenic emissions varied according to temporal profiles included in the National Emissions Inventory (NEI). They found that, when uniform temporal profiles are used on a regional scale (with 90 km resolution), the change in the weeklong average hourly ozone concentration from the time-varying emissions case over the U.S. was small during the day. Regression and frequency distribution analysis showed that the two simulations agreed well for higher ozone concentrations, but not for lower ozone concentrations. While altering all anthropogenic emissions is warranted for analyzing the overall usefulness of an inventory, this does not result in information helpful for developing emissions control strategies. Rarely are controls applied to every category of emissions. Instead regulators begin by analyzing source categories that have similar properties and then work down to specific industries or polluting processes.

In this work we continue to analyze the sensitivity of the Community Multiscale Air Quality Model (CMAQ) to altering temporal distributions of emissions, focusing on the Eastern U.S. using a 12 km grid to capture urban effects. We will look at the model's response to changing the temporal distribution individually of the four major source categories of anthropogenic emissions (area, point, on-road mobile, and non-road mobile sources) as a cursory look at the sensitivity in the model to similar emissions sources.

2. Methodology

2.1. Modeling domain

The modeling domain had 12 km grid resolution and covered the eastern half of the U.S. It was nested within a 36 km grid that covered the continental U.S. and provided the boundary conditions for the finer grid. The 36 km simulation was conducted only once, with boundary conditions provided by a global simulation with the GEOS-CHEM model. Thus each 12 km simulation had the same boundary conditions. A Lambert Conformal grid projection centered at 40N and 97W with the lower left corner located at 264 km west and 888 km south of the center defined the 12 km grid, which contained 172 × 172 grid cells. A terrain following s coordinate defined 22 layers from the surface to roughly 30 km. The top of the first layer was roughly 20 m from the surface, and the first twelve layers fell within the bottom 1.5 km of the atmosphere.

2.2. Emissions

We modeled three daily temporal profiles of emissions from area, point, on-road mobile (referred to as mobile), and non-road mobile (referred to as non-road) sources: a "uniform" temporal profile in which the emissions were the same from hour to hour, a "base" temporal profile, which utilized the temporal distribution provided in the inventories, and an "increased variability" temporal profile in which 50% of nighttime emissions were added to the daytime in order to increase the relative peak during the day and the magnitude of the daily fluctuation in emissions. The uniform and increased variability scenarios were chosen to test the limits of the models sensitivity, and are not meant to represent realistic control strategies. Biogenic emissions were not altered because known sensitivities to temperature, radiation, and relative humidity drive the diurnal variation. In total, nine simulations were conducted with different combinations of source group temporal profiles listed in Table 1. The emissions in each grid cell at any hour may be different in each simulation, but the total emissions integrated over the length of the simulation remained the same.

A 2002 emissions inventory (EI) provided by the following four regional planning organizations was processed with the Sparse Matrix Operator Kernel Emissions (SMOKE) v2.2 processor (UNC, 2008): (1) Mid-Atlantic/Northeast Visibility Union (MANE-VU), (2) Mid-West Regional Planning Organization (MRPO), (3) Visibility Improvement State and Tribal Association of the Southeast (VISTAS), and (4) Central Regional Air Planning Association (CENRAP). The 2002 EI was developed to support the 8-h ozone NAAQS attainment demonstration State Implementation Plans (SIP) in the eastern U.S. Details of the inventory and emissions processing can be found in NYSDEC (2006a, 2007) and Pechan (2006).

2.3. Meteorology

The meteorological fields were generated for the domain with the Penn State/NCAR 5th Generation Mesoscale Model 5 (MM5) v3.6 (Grell et al., 1994) by the University of Maryland in support of the 8-h ozone SIPs. Details and analysis of the simulation can be found in NYSDEC (2006b), and a brief description of the simulation details is given in Supporting Information I.

2.4. Air quality model

The emissions and meteorology were used as inputs for CMAQ v4.5 (Byun and Schere, 2006). CMAQ, a three-dimensional Eulerian grid model, simulates atmospheric chemistry, aerosol formation

Table 1
List of simulations and emissions combinations.

Run Name	Run Code	Area Temporal Profile	Point Temporal Profile	Non-road Temporal Profile	Mobile Temporal Profile
Base Case	BC	Base	Base	Base	Base
Area Uniform	AU	Uniform	Base	Base	Base
Point Uniform	PU	Base	Uniform	Base	Base
Non-road Uniform	NU	Base	Base	Uniform	Base
Mobile Uniform	MU	Base	Base	Base	Uniform
Area Increased Variability	AI	Increased Variability	Base	Base	Base
Point Increased Variability	PI	Base	Increased Variability	Base	Base
Non-road Increased Variability	NI	Base	Base	Increased Variability	Base
Mobile Increased Variability	MI	Base	Base	Base	Increased Variability

and dynamics, transport and diffusion of pollutants, and pollutant removal wet and dry processes. In this implementation, the carbon bond IV (CBIV) gas-phase chemical mechanism (Gery et al., 1989) and the AE3/ISOROPPIA aerosol reaction scheme were used along with the Euler backward iterative (EBI) solver. Daily photolysis rate constant lookup tables were generated with the JPROC processor program included in CMAQ. The Piecewise Parabolic Method was used as the horizontal advection algorithm. The simulation began on May 1st with clean initial conditions and ended on September 15. The seasonal simulation allows us to evaluate the model over different time scales and meteorological conditions (Hogrefe et al., 2000). The first 15 days were taken as spin up, and not used in the analysis.

2.5. Observational data & model performance evaluation

A model performance evaluation was carried out on the base case simulation during the 8-h NAAQS attainment demonstration SIP using a comprehensive set of measurements at the surface and aloft. Details of the assessment and a list of the various national and regional measurement networks can be found in NYSDEC (2006c). Simulated concentrations of the following species in Virginia and the Ozone Transport Region (comprised of Connecticut, Delaware, Maine, Maryland, Massachusetts, New Hampshire, New Jersey, New York, Pennsylvania, Rhode Island, Vermont, Northern Virginia, and the District of Columbia) were analyzed: O_3, particulate matter less than 2.5 mm (PM2.5), CO, NO_x, SO_2, and non-methane hydrocarbons, as well as wet deposition rates of SO_4^{2-}, NH_4^+, and NO_3^-. The threshold statistics listed in Table S1 (Supporting Information) suggested by the EPA (USEPA, 1996) for model performance evaluation were calculated for ozone when model and measurement data were paired in time and space (without interpolation). The data from July 6–9 were excluded because the model did not account for long-range transport of pollutants from forest fires in Quebec. A summary of the results from this study and the model performance evaluation conducted by Eder and Yu (2006) for the continental U.S. can be found in Supporting Information II.

3. Results

3.1. Emissions

Typical day (August 21, 2002) domain total hourly NO_x emissions are shown in Fig. 1 for the nine simulations. In Fig. 1(a), changing the diurnal variation of mobile sources to uniform (MU) has the greatest change on the domain total NO_x diurnal variation. MU case nighttime emissions increased by up to 50% and daytime emissions decreased by 10–20%. In the area uniform (AU), point uniform (PU), and non-road uniform (NU) emissions cases NO_x emissions increased by up to 10% at night and decreased by up to 4% during the day. This is expected because mobile source emissions contain the most temporal variability in the NO_x base case inventory (Fig. 2). In Fig. 1(b), increasing the temporal variation of point sources (PI) has the greatest change from the base case because point sources make up the largest fraction of the NO_x base case inventory at night (Fig. 2). The PI case has an up to 25% decrease in NO_x emissions at night, and an up to 13% increase in NO_x emissions during the day. The NO_x emissions in the other three increased variability simulations decrease by up to 8% at night and increase by up to 6% during the day. There is very little change in the domain total VOC emissions' diurnal variation when the temporal variation of the four emissions sectors are altered because biogenic emissions, which were not altered, make up 74% and 84% of the total base case VOC emissions inventory during the nighttime and daytime, respectively (Fig. 2).

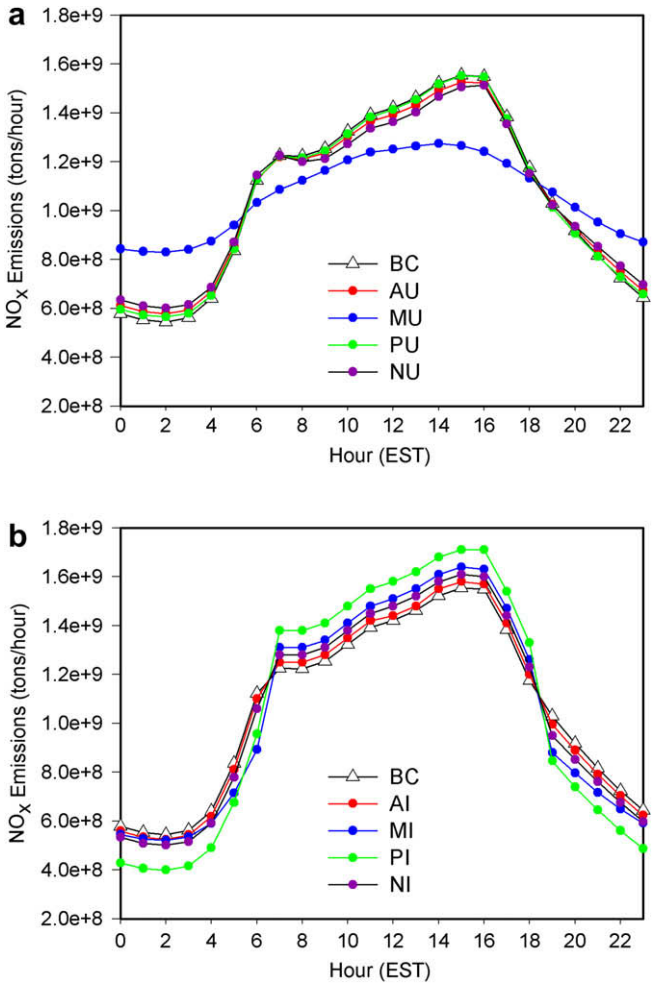

Fig. 1. The August 21, 2002 domain total hourly NO_x emissions for the (a) Base Case (BC), Area Uniform (AU), Mobile Uniform (MU), Point Uniform (PU), and Non-road Uniform (NU) simulations, and the (b) Base Case (BC), Area Increased Variability (AI), Mobile Increased Variability (MI), Point Increased Variability (PI), and Non-road Increased Variability (NI) sensitivity simulations.

3.2. Regional sensitivity to uniform temporal distributions

Deviations from the base case in the daily 8-h maximum ozone concentration (8HRMAX) by the AU, PU, MU, and NU simulations are taken to be measures of sensitivity in the model predictions to variations in the temporal distributions of the emissions sectors, assuming that the base case is a best estimate of emissions. The sensitivities are averaged over the duration of the simulation, and the largest occur when the mobile emissions' temporal distributions are made uniform (Fig. S1, Supporting Information). The domain wide average and standard deviation of the MU sensitivities were -0.4 ± 0.4 ppbv, while the AU, PU, and NU sensitivities were 0.1 ± 0.1 ppbv, -0.1 ± 0.09 ppbv, and -0.2 ± 0.2 ppbv, respectively. The sensitivities in the MU simulation have a larger area of influence than the AU, PU, and NU cases because the spatial distribution of area, point, and non-road sources varies, while motor vehicles are ubiquitous.

The average sensitivity of the 8HRMAX was also calculated for two subsets of conditions: 1) when an 8HRMAX of 50–80 ppbv occurred (moderate ozone days), and 2) when greater than 80 ppbv occurred (high ozone days) in the base case (Fig. S2). The largest sensitivities occur in the latter case (Fig. 3). In the MU simulation, on high ozone days there is a −7 ppbv (−6%) change in urban/

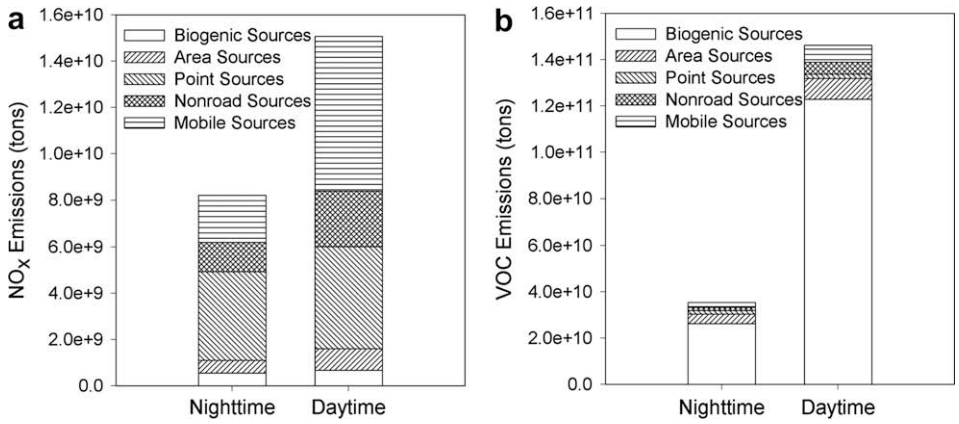

Fig. 2. The base case domain total nighttime (12:00–7:00 am EST and 7:00–12:00 pm EST) and daytime (7:00 am–7:00 pm EST) NO_x (left) and VOC (right) emissions by emissions sector on August 21, 2002.

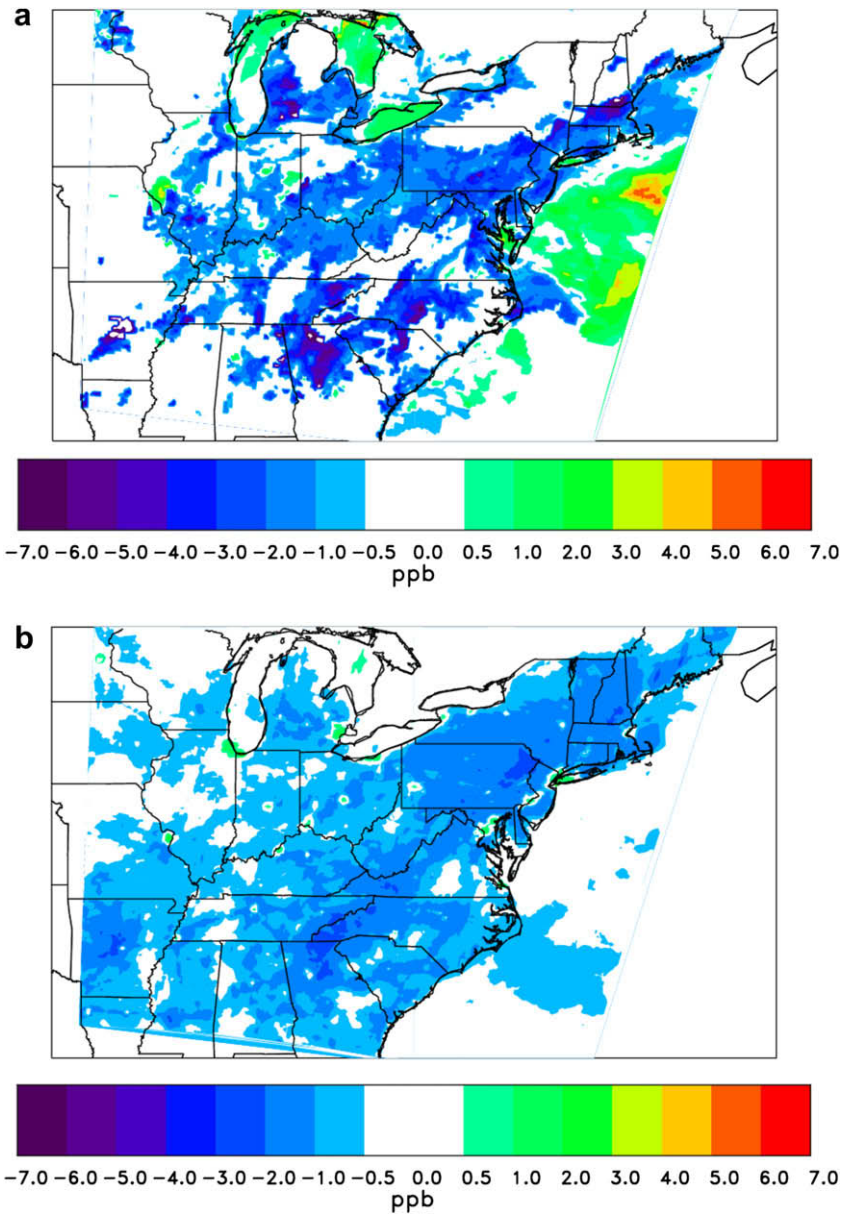

Fig. 3. The mean difference between the MU simulation and the base case $\frac{1}{N}\overset{P}{}$ Mobile uniform – base case in the daily 8HRMAX in each grid cell from May 15 to September 15 when a) greater than 80 ppbv occurs in the base case, and b) between 50 and 80 ppbv occurs in the base case.

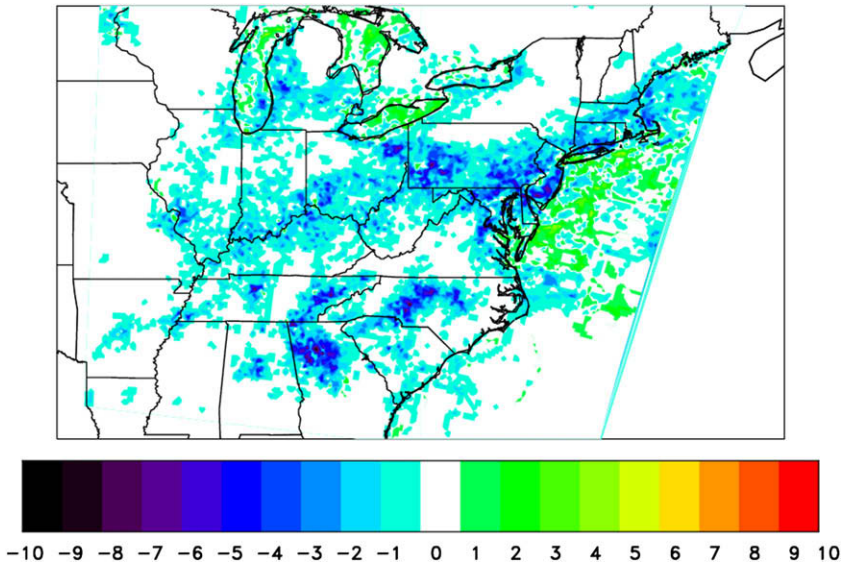

Fig. 4. The difference between the MU case and base case in the number of days that the 8HRMAX exceeds 80 ppbv from May 15 to September 15. In areas where the base case predicted 20–30 days of exceedances, the MU case predicts 5–8 less days.

suburban areas in the South, and a −3 to −4 ppbv change over most of the region. Offshore the sensitivities are +2–7 ppbv (+6%) in the North Atlantic. However, in the major city centers (e.g.; Chicago, Pittsburgh, New York City, Baltimore, Columbus, Detroit, and Indianapolis, etc.), where conditions may be VOC limited, on high ozone days a 1–2 ppb increase in the average 8HRMAX occurs because of decreased NO titration. Where the sensitivities are negative the number of days (out of the 123 day simulation) that the 8HRMAX exceeds 80 ppbv decreases by 5–8 days from 20 to 30 days in the base case (Fig. 4). Where the sensitivities are positive, the number of 80 ppbv exceedance days increases by 0–2 days.

Non-road sources had the second largest area of influence. In the NU case, over most of the East Coast, the average 8HRMAX decreases by 2–4 ppbv on high ozone days resulting in a 1–4 day decrease in 80 ppbv exceedances (Figs. S2; (c), (d) and S3; (b)).

In the AU case, along the I-95 corridor from Northern Virginia to Portland, ME, and in Alabama a 1–2 ppbv increase in the average 8HRMAX occurs on high ozone days (Fig. S2; (a), (b)). In Chicago and the middle of Kentucky, on high ozone days the 8HRMAX decreases by 1–2 ppbv, but practically no other areas in the region are affected. In the affected areas, the positive sensitivities result in 3–4 more days of 80 ppbv exceedances, and the negative sensitivities results in 1 less day of 80 ppbv exceedance (Fig. S3 (a)).

In the PU case, along the northern border of Kentucky, in the Midwest, Maryland, Delaware, and New Jersey the average 8HRMAX on high ozone days decreases by 1–3 ppbv (Fig. S2 (e), (f)). In Illinois, Missouri, Arkansas, Ohio, Pennsylvania, and Kentucky there are small areas where average 8HRMAX increases by 1–2 ppbv. The positive sensitivities occur adjacent to the negative sensitivities that are located near large point sources. Because the PU case shifts more point source emissions to the nighttime, we would expect an increase in ozone downwind of the point sources where the pollutants emitted above the nocturnal boundary layer mix down to the surface. However, the effect of downward mixing seems to only occur close to the point source. The negative sensitivities result in 1–4 less days of 80 ppbv exceedances, and the positive sensitivities result in 0–2 more days of 80 ppbv exceedances (Fig. S3; (c)).

In order to gauge the effect of the source category temporal distributions on urban areas in the region, where high ozone is a problem, we compare the 8HRMAX frequency distribution of the base case in urban and rural areas to the sensitivity runs. In this analysis, urban areas were defined as grid cells with population greater than 193 people per km^2, or 500 people per square mile, according to the year 2000 census data. The 8HRMAX frequency distributions of the AU, PU, and NU cases do not change with respect to the base case, because the sensitivity effects are too localized. In the MU case, the frequency distribution for rural areas remains similar to the base case, while in urban areas the fraction of 70–95 ppbv 8HRMAX concentrations decreases, and the fraction of 40–60 ppbv 8HRMAX concentrations in the MU simulation increases from the base case, indicating an overall downward shift in urban ozone concentrations in the region (Fig. 5).

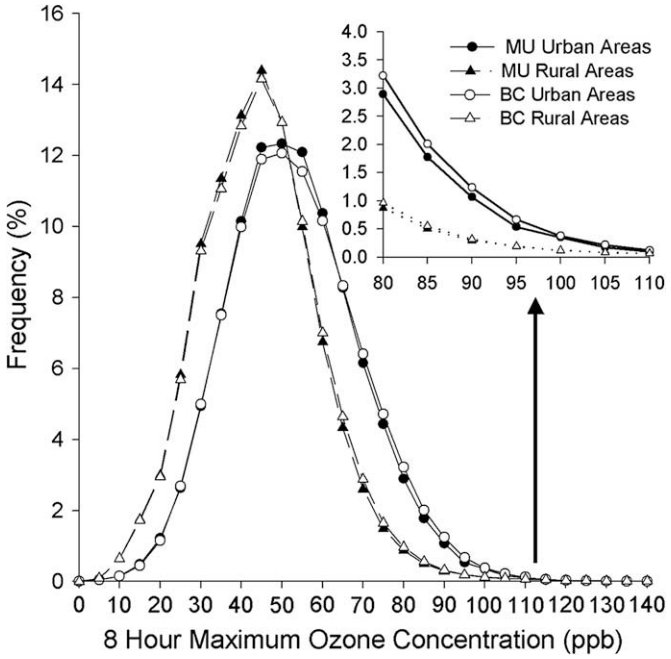

Fig. 5. The frequency distribution of the 8HRMAX in urban (circles) and rural (triangles) areas in the base case (open markers) and MU case (filled markers). The top right corner inset is an enlargement of the right tail of the frequency distribution. In urban areas the fraction of 70–95 ppbv 8HRMAX concentrations decrease, and the fraction of 40–60 ppbv 8HRMAX concentrations in the MU simulation increases from the base case.

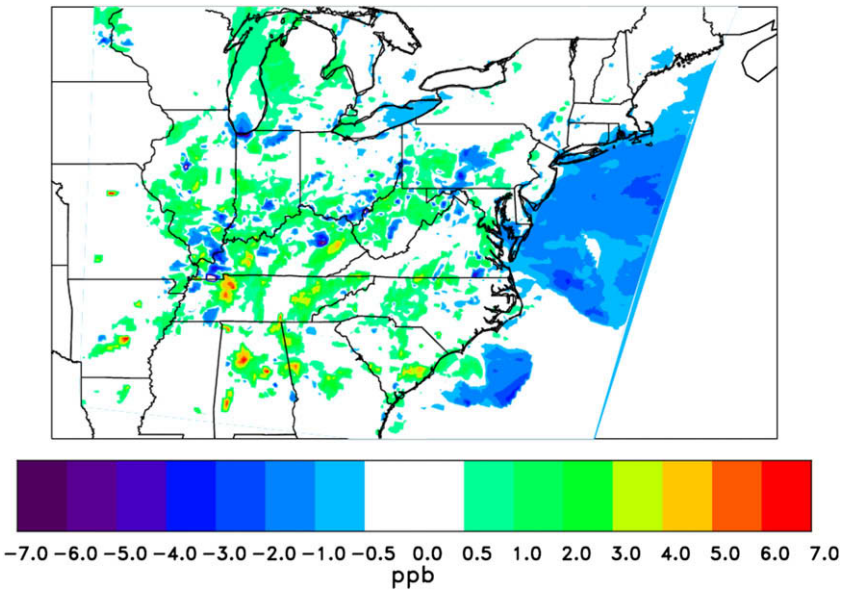

Fig. 6. The mean difference between the PI simulation and the base case in the daily 8HRMAX in each grid cell when ozone concentrations greater than 80 ppbv occur in the base case. In the Ohio River Valley, small areas of +6 and −6 ppbv sensitivity occur adjacent to each other, suggesting that, in the model, the effects of changes in emissions from the large point sources remain close to the source.

3.3. *Regional sensitivity to increased variation in temporal distributions*

When the diurnal variation of area (AI), point (PI), non-road (NI), and mobile (MI) emissions is increased, smaller sensitivities than the uniform cases are observed (Fig. S4). The increased temporal variability of area sources has very little effect; the map of sensitivities shows less than 1 ppbv change throughout the domain (Figs. S4 (a) and S5 (a), (b)).

In the (NI) case the domain wide average 8HRMAX sensitivity is 0.06 ± 0.1 ppbv. However, in the Ohio River Valley, West Virginia, and Kentucky the average 8HRMAX decreases by 2–3 ppbv on high ozone days (Fig. S5 (d)). In the south, the 8HRMAX increases by 1–2 ppbv on high ozone days. These sensitivities result in 1–3 less and 1–2 more 80 ppbv exceedances, respectively (Fig. S6 (b)).

In the MI case, the domain wide average 8HRMAX sensitivity is 0.09 ± 0.2 ppbv. Throughout the domain, the average 8HRMAX increases by 1–2 ppbv on high ozone days, and up to 5 more exceedances than the base case of 80 ppbv occur (Figs. S5 (f) and S6 (c)). However, the rural and urban frequency distributions of the 8HRMAX for the MI case do not significantly change from the base case.

Increasing the temporal variation of point source (PI) emissions also results in small domain wide sensitivities: 0.04 ± 0.3 ppbv. Larger localized sensitivities on high ozone days on the order of +6 ppbv occur near Atlanta, Birmingham, Knoxville, and Nashville (Fig. 6). In the Ohio River Valley, Indiana, Illinois, Tennessee, and Kentucky, small areas of positive 1–6 ppbv and negative 1–5 ppbv sensitivity occur adjacent to each other, suggesting that, similar to the PU case, the effects of changes in emissions from the large point sources located in this region for the most part remain close to the source. Because the PI case increases point source emissions during the daytime, one might expect that ozone would decrease at the location of the large point sources because of NO_x titration. However, in these areas there is enough isoprene such that conditions are NO_x limited (Fig. S7).

This result, along with the PU case, is in agreement with the spatial correlation analysis conducted by Gilliland et al. (2008). They found that when point source emissions are changed according to measurements before and after the NO_x SIP Call, the subsequent changes in model ozone concentrations are a result of changes in emissions sources that are close by rather than transported emissions. However, a comparison of CMAQ to ground observations shows that CMAQ underestimates the ozone e-folding distance; the observed effects of the point source emissions changes were more wide spread than the model predicts. This corroborates similar finding by Kim et al. (2006), Hains et al. (2008), and Bloomer et al. (2009) and suggests if the model were able to simulate pollutant transport as seen in the observations, the area

Fig. 7. The location of the PAMS type 2 (triangles), PAMS type 3 (squares), and CASTNET (circles) monitoring sites used for local sensitivity analysis in Baltimore (top) and Atlanta (bottom).

and magnitude of the sensitivities in the PI and PU simulations would be larger.

3.4. Local sensitivities

Baltimore and Atlanta were selected for further analysis based on the results of the regional sensitivities. Average hourly ozone measurements at three monitoring sites near each of the cities were compared to each of the sensitivity simulations: two monitoring sites within the Photochemical Assessment Monitoring Stations (PAMS) network, and one within the Clean Air Status and Trends Network (CASTNET). The CASTNET sites, Arendtsville (site id: ARE128) near Baltimore and Sand Mountain (site id: SND152) near Atlanta, provide data on rural ozone levels. The PAMS monitoring stations are located within and downwind of polluted areas where emissions of precursors and their effects can be observed. Essex (site id: 24-005-3001) and Tucker (site id: 13-089-3001) are the PAMS type 2 sites for Baltimore and Atlanta, respectively, and are located within the area of maximum emissions levels. Aldino (site id: 24-025-9001) and Conyers (site id: 13-247-0001) are the PAMS type 3 sites, and lie predominantly downwind of Baltimore and Atlanta, respectively. A map of the locations of the six selected sites is shown in Fig. 7. Site descriptions can be found at http://www.epa.gov/oar/oaqps/pams/ and http://www.epa.gov/castnet.

Overall, the largest effect on the modeled hourly ozone values at the selected monitoring sites occurs at night when mobile emissions are temporally uniform. The increased nighttime emissions from the mobile source group, which are rich in NO_x, in the MU case, build up locally during typically stagnant conditions and destroy ozone via NO_x titration. Thus, at the Essex and Tucker sites, the MU simulation causes hourly ozone values at night to decrease from the base case by up to 10 ppbv. Yet, compared to observations, the MU simulation has better model performance at night than the base case (Fig. 8 (a,c)). Conversely, when mobile source temporal variations are increased and NO_x emissions decrease at night, at these sites, the MI simulation nighttime ozone values are slightly higher than the base case (Fig. 8 (b,d)).

At the Aldino site, the nighttime hourly ozone values predicted in the base case are close to measurements. Thus, increasing NO_x emissions at night in the MU simulation results in underestimated ozone. Also, the model predicts the ozone maximum 1 h earlier than the measurements at this site. When the diurnal variation of the emissions is changed in the sensitivity simulations, there is no change in when the peak ozone values occurs (Fig. S8 (a), (b)). At the Conyers site, similar to the Tucker site, the model reproduces the diurnal variation of ozone, but overestimates ozone at night. Likewise, the MU simulation lowers the nighttime ozone concentrations from the base case at this site, although ozone predictions remain w 10 ppbv greater than observations (Fig. S8 (c)).

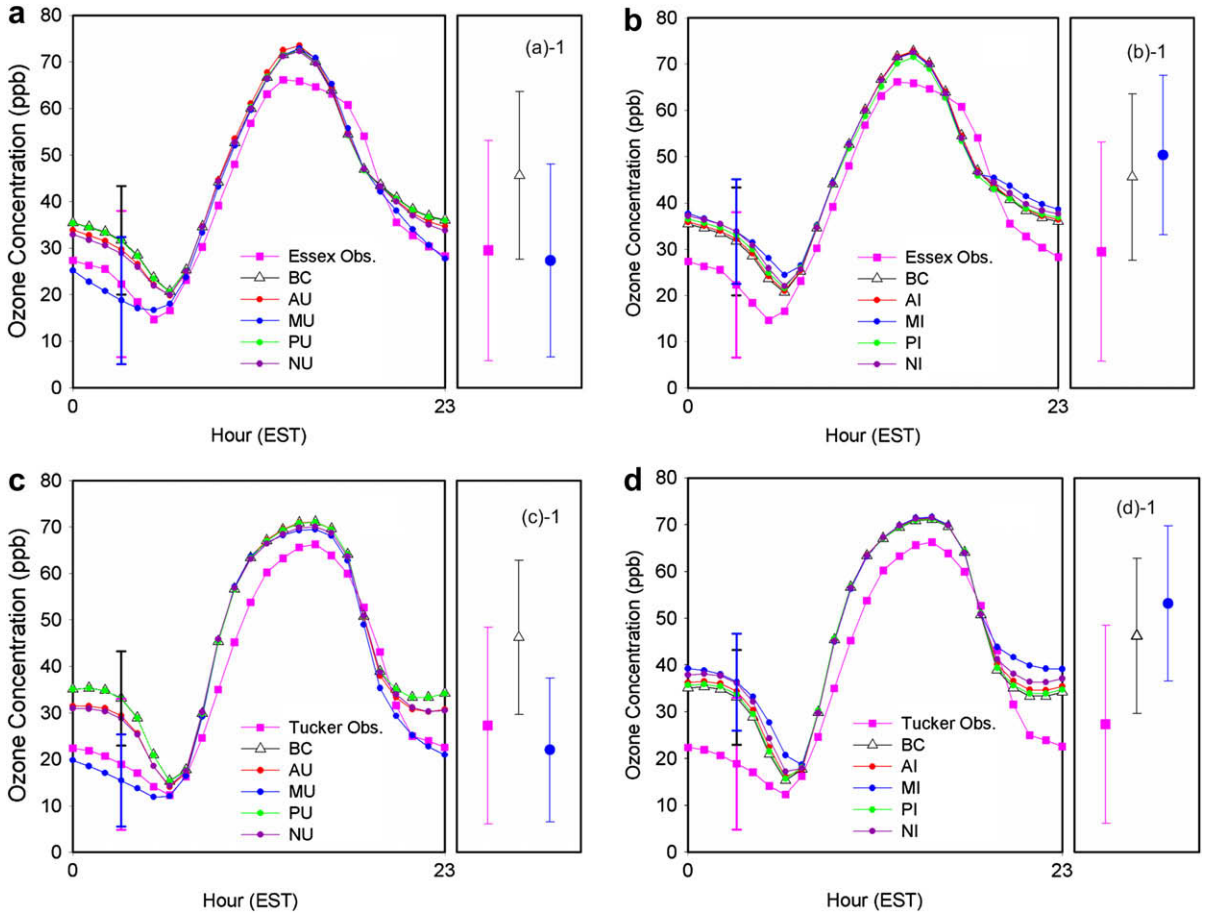

Fig. 8. The hourly ozone concentrations averaged in time that were observed (pink squares) and modeled at the Essex (a, b) and Tucker (c, d) monitoring sites. The modeled average hourly ozone concentration plots are separated into uniform (left column) and increased variability (right column) groups. The base case (open triangles) is plotted with both groups. The error bars on the fourth point in each figure correspond to the standard deviation of the observed (pink), base case (black), and mobile case (blue) hourly ozone concentrations, and are typical for all hours. The plot to the right of each diel plot (a-1, b-1, c-1, d-1) is a magnification of these points next to each other to better illustrate the over lapping error bars. At the Essex and Tucker sites, the summer long average decrease from the base case in nocturnal ozone when mobile emissions are uniform is larger than one standard deviation. (For interpretation of the references to colour in this figure legend, the reader is referred to the web version of this article.)

In order for the AQM to capture the diurnal variation of observed ozone, especially the nighttime minimum, first the meteorological model must reproduce the diurnal variation of the planetary boundary layer (PBL). Unfortunately, few temporally and spatially detailed boundary layer observation datasets exist that can be used to validate model results. However, Rao et al. (2003) were able to evaluate the mixing height from a 1995 MM5 simulation using the Blackadar PBL scheme with sounding data from the North American Research Strategy for Tropospheric Ozone-Northeast (NARSTO-NE) (Berman et al., 1999) field program and found good agreement at night. Additionally, it has been shown that the modified Blackadar scheme used in this work is best suited for simulating diurnal cycles of surface wind speed in relation to surface temperature (Zhang and Zheng, 2004). Although the Rao et al. (2003) comparison is for a different model year than this study, because MM5 has acceptable model performance for the other observed meteorological variables in this work, we will assume our simulation does a reasonable job at reproducing nocturnal mixing heights. It follows that the overestimation of nighttime ozone by the base case at the PAMS type 2 sites may be the result of another weakness in the model.

One cause of some of the overestimation of nocturnal ozone by the model may be the strong gradient in ozone concentration near the surface. The model value represents the concentration at the mid-layer height (10 m), while the observations are made at 5 m. The lower nighttime ozone values at the Essex and Tucker sites in the temporally uniform simulations, especially the MU case, suggest that underestimated NO_x emissions and/or overestimated losses of NO_x at night may also play a role in the nighttime over prediction of ozone by CMAQ in urban areas. This reasoning seems appropriate for the Essex site where the NO_x model performance improves in the MU case. The base case underestimates observed nighttime NO_x concentrations by 38%, while the MU case underestimates nighttime NO_x by 10%. However, at the Tucker site, the base case nighttime NO_x concentrations agree well with observations, except for over predictions from 19:00 to 21:00 local time, while the MU case over predicts nighttime NO_x observations by 95% (Fig. S9).

At the rural CASTNET sites, Arendtsville and Sand Mountain, the model has a low bias during the day (Fig. S10). At night, the model underestimates ozone over Arendtsville, and overestimates ozone over Sand Mountain. Regardless, the sensitivity simulations have very little effect on the performance of the model at these rural sites. The low daytime bias may be due to the reaction rate of the hydroxyl radical with NO_2 in CBIV that terminates the hydroxyl radical too quickly during the daytime and inhibits the production of ozone through the oxidation of aldehydes (Faraji et al., 2008). This mechanism would be important in rural areas where VOCs from biogenic emissions dominate.

4. Discussion and implications

Mobile emissions have the largest temporal variation in the base case emissions inventory. Making the temporal variation of this source group uniform caused the largest effects on the 8HRMAX. Particularly, the 8HRMAX decreased in urban areas on days with high (greater than 80 ppbv) ozone by up to 7 ppbv, resulting in a decrease in the number of 80 ppbv exceedances. This result has significant policy implications in terms of calculating relative reductions for demonstrating attainment with the NAAQS. From a regulatory perspective, the decrease in the number of 80 ppbv exceedances in the MU simulations demonstrates that accurate representation of daily variability of mobile emissions is necessary to simulate ozone correctly. The other emissions source groups also affected the number of 80 ppbv exceedances, but on a more local level. This reinforces the importance of understanding local emissions characteristics in order to compose effective ozone abatement strategies.

The results from the MU case also demonstrate the upper limits of intentionally shifting traffic patterns as an abatement strategy. If traffic emissions occurred more at night and less in the day, there would be fewer ozone events. Such a temporal shift might be accomplished by switching to electric cars charged at night, or increasing the number of high occupancy vehicle lanes in a metropolitan region, which would force commuters to drive at off peak hours. In fact, if a larger fraction of the vehicle fleet became electric cars, an even greater decrease in ozone could occur because overall NO_x emissions should decrease (total emissions from power plants are capped, while emissions from cars are limited by the per vehicle miles traveled).

Because point sources are the largest nighttime emitters in the base case emissions inventory, increasing the temporal variation of this source group has the greatest effect. Similar to the result from the PU case, changes in the 8HRMAX and the number of 80 ppbv exceedances mostly occur close to the emissions sources. The patchy result of positive and negative sensitivities close to each other may be due to the weakness of the model at transporting point source emissions, which underestimates the area and magnitude of ozone generated by point source emissions. Because of this weakness the model appears to be able to respond more realistically to emissions control strategies that target the time of day of emissions from mobile, area, and non-road sources, than from point sources.

We find from comparisons at several monitors that the largest differences between the base case and temporal sensitivity simulations occur in the nighttime (similar to Tao et al. (2004)), especially in urban areas when the mobile emissions temporal distribution is uniform. Model performance is poor at night, but improves in urban areas when mobile emissions are made uniform in time. Correcting model underestimated nighttime NO_x emissions and/or overestimated NO_x losses will enhance the numerical simulation of ozone and our ability to evaluate pollution abatement strategies. Adequate treatment by the model of the night-to-day ozone accumulation process is essential to photochemical modeling (Rao et al., 2003), and will become especially important as emissions and ozone concentrations decrease.

Acknowledgements

We would like to thank Dale Allen for his assistance with data visualization, and for providing the base case modeling results. This research has been funded by the Maryland Department of Environment.

Appendix A. Supplementary information

Supplementary data associated with this article can be found, in the online version, at doi:10.1016/j.atmosenv.2009.05.045

References

Appel, K.W., Gilliland, A.B., Sarwar, G., Gilliam, R.C., 2007. Evaluation of the Community Multiscale Air Quality (CMAQ) model version 4.5: sensitivities impacting model performance Part I-Ozone. Atmospheric Environment 41, 9603–9615.

Arnold, J.R., Dennis, R.L., 2006. Testing CMAQ chemistry sensitivities in base case and emissions control runs at SEARCH and SOS99 surface sites in the southeastern US. Atmospheric Environment 40, 5027–5040.

Berman, S., Ku, J.Y., Rao, S.T., 1999. Spatial and temporal variation in the mixing depth over the Northeastern United States during the summer of 1995. Journal of Applied Meteorology 38 (12), 1661–1673.

Bey, I.J., D.J., Yantosca, R.M., Logan, J.A., Field, B.D., Fiore, A.M., Li, Q.B., Liu, H.G.Y., Mickley, L.J., Schultz, M.G., 2001. Global modeling of tropospheric chemistry with assimilated meteorology: model description and evaluation. Journal of Geophysical Research 106 (D19), 23073–23095.

Bloomer, B.J., Stehr, J.W., Piety, C.A., Salawitch, R.J., Dickerson, R.R., 2009. Observed relationships of ozone air pollution with temperature and emissions. Geophysical Research Letters 36, L09803. doi:10.1029/2009GL037308.

Brunner, D.S., Staehelin, J., Rogers, H.L., Kohler, M.O., Pyle, J.A., Hauglustaine, D.A., Jourdain, L., Berntsen, T.K., Gauss, M., Isaksen, I.S.A., Meijer, E., van Velthoven, P., Pitari, G., Mancini, E., Grewe, V., Sausen, R., 2005. An evaluation of the performance of chemistry transport models – part 2: detailed comparison with two selected campaigns. Atmospheric Chemistry and Physics 5, 107–129.

Byun, D., Schere, K.L., 2006. Review of the governing equations, computational algorithms, and other components of the models-3 community multiscale air quality (CMAQ) modeling system. Applied Mechanics Reviews 59, 51–77.

Eder, B., Yu, S., 2006. A performance evaluation of the 2004 release of Models-3 CMAQ. Atmospheric Environment 40 (26), 4811–4824.

Faraji, M., Kimura, Y., McDonald-Buller, E., Allen, D., 2008. Comparison of the carbon bond and SAPRC photochemical mechanisms under conditions relevant to southeast Texas. Atmospheric Environment 42, 5821–5836.

Fine, J., Vuilleumier, L., Reynolds, S., Roth, P., Brown, N., 2003. Evaluating Uncertainties in regional photochemical air quality modeling. Annual Review of Environment and Resources 28, 59–106.

Gego, E., Gilliland, A., Godowitch, J., Rao, S.T., Porter, P.S., Hogrefe, C., 2008. Modeling analyses of the effects of changes in nitrogen oxides emissions from the electric power sector on ozone levels in the eastern United States. Journal of the Air & Waste Management Association 58, 580–588.

Gery, M.W., Whitten, G.Z., Killus, J.P., Dodge, M.C., 1989. A photochemical kinetics mechanism for urban and regional scale computer modeling. Journal of Geophysical Research 94 (D10), 12,925–12,956.

Gilliland, A.B., Hogrefe, C., Pinder, R.W., Godowitch, J.M., Foley, K.L., Rao, S.T., 2008. Dynamic evaluation of regional air quality models: assessing changes in O_3 stemming from changes in emissions and meteorology. Atmospheric Environment 42, 5110–5123.

Godowitch, J.M., Gilliland, A.B., Draxler, R.R., Rao, S.T., 2008. Modeling assessment of point source NO_x emission reductions on ozone air quality in the eastern United States. Atmospheric Environment 42 (1), 87–100.

Grell, G.A., Dudhia, J., Stauffer, D.R., 1994. A description of the 5th generation Penn State/NCAR Mesoscale Model (MM5), NCAR Technical Note 398+STR.

Hains, J.C., Taubman, B.F., Thompson, A.M., Marufu, L.T., Stehr, J.W., Dickerson, R.R., 2008. Origins of chemical pollution derived from mid-Atlantic aircraft profiles using a clustering technique. Journal of Geophysical Research 42 (8), 1727–1741.

Hanna, S.R., Chang, J.C., Fernau, M.E., 1998. Monte Carlo estimates of uncertainties in predictions by a photochemical grid model (UAM-IV) due to uncertainties in input variables. Atmospheric Environment 32 (21), 3619–3628.

Hogrefe, C., Rao, S.T., Zurbenko, I.G., Porter, P.S., 2000. Interpreting the information in ozone observations and model predictions relevant to regulatory policies in the Eastern United States. Bulletin of the American Meteorological Society 81 (9), 2083–2106.

Kim, S.W., Heckel, A., McKeen, S.A., Frost, G.J., Hsie, E.Y., Trainer, M.K., Richter, A., Burrows, J.P., Peckham, S.E., Grell, G.A., 2006. Satellite-observed US power plant NO_x emission reductions and their impact on air quality. Geophysical Research Letters 33, L22812.

Mallet, V., Sportisse, B., 2006. Uncertainty in a chemistry-transport model due to physical parameterizations and numerical approximations: an ensemble approach applied to ozone modeling. Journal of Geophysical Research 111, D01302.

Marr, L.C., Black, D.R., Harley, R.A., 2002. Formation of photochemical air pollution in central California: 1. Development of a revised motor vehicle emission inventory. Journal of Geophysical Research 107 (D6), 4047.

Murphy, C.F., Allen, D.T., 2005. Hydrocarbon emissions from industrial release events in the Houston–Galveston area and their impact on ozone formation. Atmospheric Environment 39, 3785–3798.

Nam, J., Webster, M., Kimura, Y., Jeffries, H., Vizuete, W., Allen, D.T., 2008. Reductions in ozone concentration due to controls on variability in industrial flare emissions in Houston, Texas. Atmospheric Environment 42, 4198–4211.

New York State Department of Environmental Conservation (NYSDEC), 2006a. Processing of Biogenic Emissions for OTC/MANE-VU Modeling, TSD-1b. http://www.dec.ny.gov/docs/air_pdf/POK5final.pdf.

New York State Department of Environmental Conservation (NYSDEC), 2006b. Meteorological Modeling Using Penn State /NCAR 5th Generation Mesoscale Model (MM5). http://www.dec.ny.gov/docs/air_pdf/POK4final.pdf> .

New York State Department of Environmental Conservation (NYSDEC), March 2006c. CMAQ Model Performance and Assessment 8-h OTC Ozone Modeling. http://www.dec.ny.gov/docs/air_pdf/POK6final.pdf.

New York State Department of Environmental Conservation (NYSDEC), 2007. Emissions Processing for 2002 OTC Regional and Urban 12 km Base Year Simulation, TSD-1c. http://www.dec.ny.gov/docs/air_pdf/POK5final.pdf.

Pechan, E.H., Associates, Inc. (Pechan), Nov 2006. Technical Support Document for 2002 MANE-VU SIP Modeling Inventories version 3, Final Report to the Mid-Atlantic/Northeast Visibility Union. http://www.ct.gov/dep/lib/dep/air/regulations/sip/regionalhaze/m_mane-vu_final_v3_tsd_11-20-06.pdf> .

Placet, M., Mann, C.O., Gilbert, R.O., Niefer, M.J., 2000. Emissions of ozone precursors from stationary sources: a critical review. Atmospheric Environment 34, 2183–2204.

Rao, S.T., Ku, J.Y., Berman, S., Zhang, K., Mao, H., 2003. Summertime characteristics of the atmospheric boundary layer and relationships to ozone levels over the eastern United States. Pure and Applied Geophysics 160, 21–55.

Seinfeld, J.H., Pandis, S.N., 2006. Atmospheric Chemistry and Physics: from Air Pollution to Climate Change. Wiley & Sons, New York.

Tao, Z., Larson, S.M., Williams, A., Caughey, M., Wuebbles, D.J., 2004. Sensitivity of regional ozone concentrations to temporal distribution of emissions. Atmospheric Environment 38, 6279–6285.

University of North Carolina (UNC), 2008. SMOKE v2.2 User's Manual. http://www.smoke-model.org/version2.2/index.cfm (accessed Dec 2008).

U.S. Environmental Protection Agency (USEPA), 1996. Compilation of Photochemical Models' Performance Statistic for 11/94 Ozone SIP Applications. USEPA, Office of Air Quality Planning and Standards, Research Triangle Park, NC 27711, 156. EPA-454/R-96-004.

U.S. Environmental Protection Agency (USEPA), 2004. The Ozone Report: Measuring Progress through 2003, 454/K-04-001. Office of Air Quality Planning and Standards, Emissions Monitoring and Analysis Division, U.S. Environmental Protection Agency, Research Triangle Park, NC 27711.

Webster, M., Nam, J., Kimura, Y., Jeffries, H., Vizuete, W., Allen, D.T., 2007. The effect of variability in industrial emissions on ozone formation in Houston, Texas. Atmospheric Environment 41, 9580–9593.

Zhang, D.L., Zheng, W.Z., 2004. Diurnal cycles of surface winds and temperatures as simulated by five boundary layer parameterizations. Journal of Applied Meteorology 43 (1), 157–169.